Saturated Pressure and *P*−*V*−*T* Measurements for 1,1,1,3,3,3-Hexafluoropropane (R-236fa)

Giovanni Di Nicola, Giuliano Giuliani, and Fabio Polonara*

Department of Energetics, University of Ancona, Via Brecce Bianche, 60100 Ancona, Italy

Roman Stryjek

Institute of Physical Chemistry, Polish Academy of Sciences, ul. Kasprzaka 44/52, 01-224 Warsaw, Poland

Saturated pressure and *P*−*V*−*T* measurements were performed for 1,1,1,3,3,3-hexafluoropropane (R-236fa) in a constant volume cell. The saturated pressure measurements covered a temperature range from 248 K up to 360 K and a corresponding pressure range from 34 kPa up to 1472 kPa. The results were fitted to various empirical equations. The *P*−*V*−*T* measurements in the superheated vapor region were made along seven isochores from 314 K up to 364 K and from 405 kPa up to 998 kPa. The *P*−*V*-*T* data were regressed to the virial equation of state in the Leiden form truncated after the third term. A valid consistency of the derived second virial coefficients was shown using the Tsonopoulos and the Weber correlating methods. In the results of our measurements, 113 data points were collected, 71 and 42 of which were obtained, respectively, for the saturated pressure and superheated region.

Introduction

R-236fa has a low ozone depletion potential and seems a promising substitute for compounds containing chlorine in high-temperature heat pumps, in chemical blowing agents for use in the manufacture of polyurethane and phenolic resin foams, and as a component of cleaning fluids, fire suppressants, and propellants. These are just a few examples of its potential industrial applications described in the literature. Several of its physical and thermodynamic properties have been the object of research, including reports on its viscosity in saturated conditions (Laesecke and Defibaugh, 1996) and on its heat capacities and entropies (Hwang et al., 1992). An equation of state for the thermodynamic properties (Outcalt and McLinden, 1995) has been proposed. Recent publications have dealt with certain physical properties (Schmidt et al., 1996), the speed of sound (Gilles, 1997), and dipole moment (Goodwin and Mehl, 1997).

Apart from some data on saturation pressure (Bobbo et al., 1998 and Basile, 1998), no reports have been published in the open literature, to our knowledge, on experimental saturated pressures and volumetric properties; the study presented in this paper aims to partially fill this gap.

Experimental Section

Reagent. The sample was provided by DuPont of Nemours; its purity was checked by gas chromatographic analysis, and we found 99.94% on an area response basis using a thermal conductivity detector.

Apparatus. A classical constant-volume apparatus with a volume of around 254 cm^3 was used. Details of the apparatus are already described elsewhere (Giuliani et al., 1995a; Giuliani et al., 1995b) and are omitted here, where the most essential information is given with a more detailed description of the main modifications made to the charging system. The experimental apparatus is schematically illustrated in Figure 1. A spherical stainless steel AISI 304 cell containing refrigerant is connected to a differential diaphragm pressure transducer, coupled to an electronic null indicator. The spherical cell and the pressure transducer are immersed in the main thermostatic bath containing a mixture of water and glycol and controlled by a PID device. An auxiliary bath, also controlled by a PID device, helps the system to keep the temperature constant. The temperature is measured with a platinum resistance thermometer immersed near the cell. The instrument is calibrated according to ITS-90, and its uncertainty is certified as being within ±15 mK. The pressure measurement is obtained with a dead weight gage, and the experimental uncertainty in the pressure measurements can be estimated to be within ±0.5 kPa.

To reduce the uncertainty in the measurement of the mass of the sample loaded into the cell, the compound is first put into a small bottle and weighed using an analytical balance (uncertainty ±0.3 mg). Then, after emptying the cell and the connections, the bottle is discharged into the sphere without taking it out of the bath. At the end of this operation, the bottle is weighed and the uncertainty in the measurement of the mass is calculated directly from the difference between the two weights. Finally, the mass remaining inside the duct during the charging procedure is estimated and subtracted from the total mass of the charge.

In the overall uncertainty in the measurement of the mass inside the cell, both the uncertainties in the estimate of the mass inside the duct and the uncertainties stemming from the difference between the two weights are taken into account. For a one-component system, an overall uncertainty of ±8.5 mg was obtained.

The volume of the cell, the piping, and the cavity of the pressure transducer is measured with an uncertainty of

* Corresponding author. Phone: +39-0712204432. Fax: +39-071280-4239. E-mail: polonara@popcsi.unian.it.

10.1021/je980281e CCC: $18.00 © 1999 American Chemical Society
Published on Web 05/15/1999

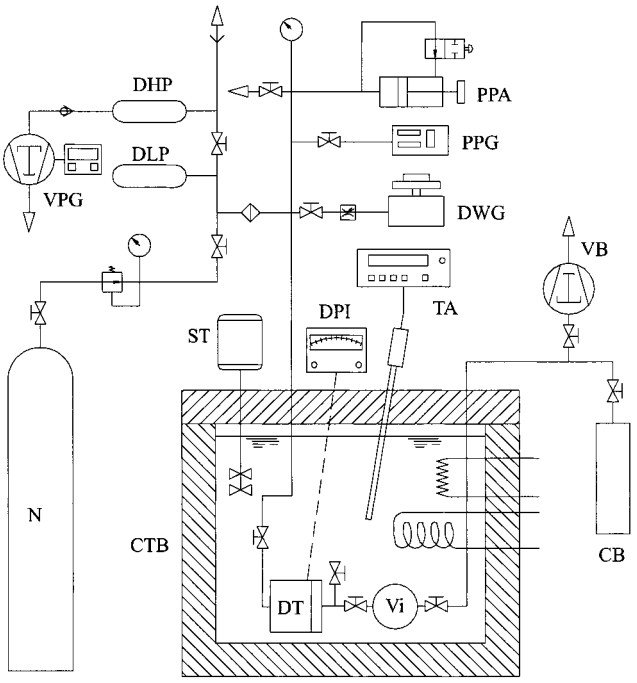

Figure 1. Schematic diagram of the apparatus: CTB, thermostatic bath; DHP, high-pressure expansion chamber; DLP, low-pressure expansion chamber; DPI, electronic null indicator (Ruska, mod. 2461); DT, pressure differential transducer (Ruska, mod. 2413); DWG, dead weight gauge (Ruska, mod. 2465); N, nitrogen reservoir; PPA, precision pressure controller (Ruska, mod. 3891); PPG, vibrating cylinder pressure gauge (Ruska, mod. 6220); ST, stirrer; TA, platinum resistance thermometer (Minco, mod. S7929, + Franco Corradi, mod. RP700); Vi, constant volume spherical cell; VP, vacuum pump (Vacuubrand, mod. RZ2); VPG, vacuum pump gauge (Galileo, mod. OG510); CB, charging bottle.

± 0.0003 dm^3. From the uncertainties in mass and volume measurements, the uncertainty in calculated molar volume was estimated to always be lower than ± 0.002 dm^3 mol^{-1}.

From the single uncertainties, the overall experimental uncertainty in terms of pressure, calculated using the laws of error propagation, was estimated to be lower than ± 0.6 kPa for measurements along the saturation line and lower than 1.1 kPa in the superheated vapor region.

Results and Discussion

Vapor Pressure. The experimental vapor pressures within a temperature range from 248 K to 360 K are given in Table 1; these values were fitted to various empirical equations. One of the most popular is the Antoine equation presented below,

$$\log P/\mathrm{kPa} = A - B/(C + T/\mathrm{K}) \qquad (1)$$

where P is the pressure and T is the temperature. From the results of the data fit, the following values were found for the parameters: $A = 6.255888$, $B = 1004.490$, $C = -35.332$, with $\mathrm{d}P = 0.00$ and $\mathrm{abs}(\mathrm{d}P) = 0.12$, where the percentage deviations in pressure are defined as

$$\mathrm{d}P = \frac{1}{n}\sum_{i=1}^{n}[(P_{\mathrm{exp}} - P_{\mathrm{calc}})/P_{\mathrm{exp}} \times 100] \qquad (2)$$

$$\mathrm{abs}(\mathrm{d}P) = \frac{1}{n}\sum_{i=1}^{n}[\mathrm{abs}(P_{\mathrm{exp}} - P_{\mathrm{calc}})/P_{\mathrm{exp}} \times 100] \qquad (3)$$

where n is the number of experimental points. The deviations from the fit for each datum point are presented in Figure 2. An S-shaped distribution is apparent, showing that the three-parameter Antoine equation is unable to represent the saturated pressure accurately for this temperature and pressure range. To improve eq 1, various modifications using more than three parameters are described in the literature. We used a four-parameter equation in the following form:

$$\ln P/\mathrm{kPa} = A - B/(C + T/\mathrm{K}) + D \ln(T/\mathrm{K}) \qquad (4)$$

From the results of the fit, we obtained the following values for the parameters: $A = -2.3085025$, $B = 1271.174$, $C = -74.380$, and $D = 2.385$, with $\mathrm{d}P = -0.003$ and $\mathrm{abs}(\mathrm{d}P) = 0.076$. The scatter diagram of the deviations presented in Figure 3 shows that its random distribution is within our estimated experimental uncertainty. The data from Bobbo et al., 1998 and from Basile, 1998 are also shown in this figure and compared with eq 4, showing good consistency among the data.

Another empirical equation for saturated pressure representation has been proposed by Wagner and Setzmann (1991),

$$\ln P_{\mathrm{r}} = \left(\frac{1}{T_{\mathrm{r}}}\right)\sum_{i=1}^{21} a_i(1 - T_{\mathrm{r}})^{i/2} \qquad (5)$$

Table 1. Experimental Saturation Pressures for R-236fa

T_{90}/K	P/kPa	T_{90}/K	P/kPa	T_{90}/K	P/kPa
247.99	33.9	293.99	235.6	316.57	482.6
253.01	43.7	294.66	241.5	317.26	492.2
253.65	45.1	295.36	247.7	318.41	508.8
258.19	56.0	298.27	272.5	319.02	518.4
263.17	70.4	298.97	279.1	322.31	568.6
263.73	72.0	299.04	279.9	323.41	585.9
263.77	72.3	303.19	320.3	323.70	592.4
267.96	86.8	303.26	321.1	323.73	591.2
273.15	107.7	303.32	321.9	323.75	592.8
273.29	108.5	303.59	325.3	328.12	668.0
274.04	111.6	303.66	325.2	330.47	712.1
274.76	115.1	303.75	326.5	332.84	758.0
278.84	135.6	304.64	335.9	333.37	767.7
283.12	159.5	307.08	361.9	333.69	773.7
283.18	159.8	308.67	380.7	335.41	810.1
283.30	160.4	309.05	385.2	338.29	871.0
283.61	162.6	310.21	399.0	342.68	972.5
283.89	164.4	313.38	439.5	343.30	986.6
288.91	197.5	313.75	445.3	346.21	1059.0
289.00	197.8	313.82	445.7	348.63	1121.8
290.64	210.0	313.92	446.3	348.88	1130.0
293.54	232.2	314.03	448.1	353.53	1257.6
293.71	233.7	314.10	448.8	360.42	1471.8
293.88	234.9	314.18	449.2		

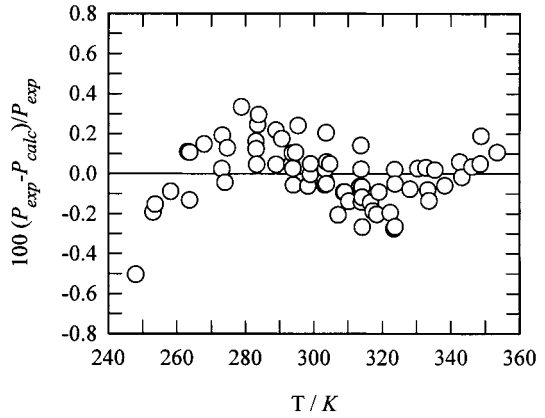

Figure 2. Scatter diagram of the saturated pressure deviations from the fit with the Antoine equation, eq 1.

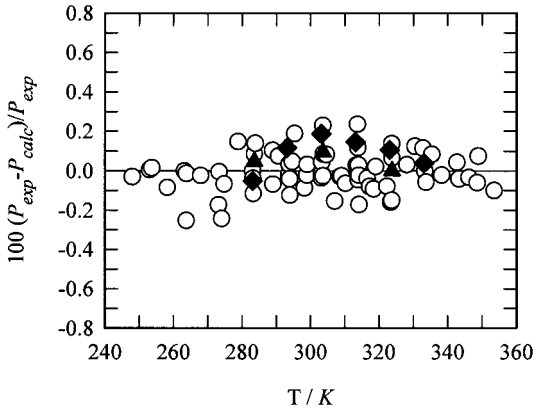

Figure 3. Scatter diagram of the saturated pressure deviations from the fit with eq 2 and comparison with Bobbo et al., 1997 (▲) and Basile, 1998 (◆) data.

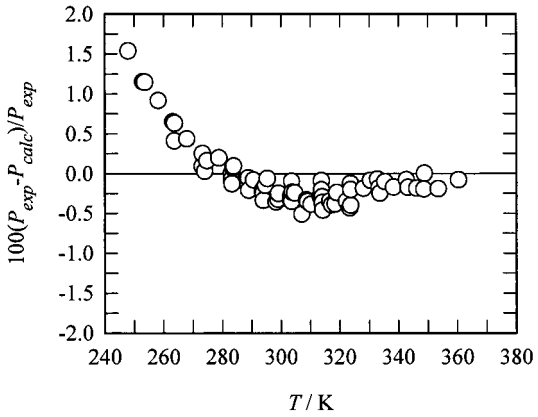

Figure 4. Scatter diagram of deviations between experimental saturated pressures and values calculated the MBWR EOS (McLinden et al., 1998).

where $P_r = P/P_c$ and $T_r = T/T_c$, with the critical pressure, $P_c = 3200$ kPa, and the critical temperature, $T_c = 398.07$ K, adopted from McLinden et al., 1998. Various forms of eq 5 are used in the literature, leading to a great flexibility in the use of the equation. Various values are also proposed for the exponents in eq 5. Here, we ran preliminary tests on a few versions proposed in the literature with three or four adjustable parameters and various values of the exponents, considering one of the major advantages of the Wagner equation, i.e., that it can be extrapolated up to the critical point. We found that the equation in the following form:

$$\ln P_r = \left(\frac{1}{T_r}\right)(a_0 T_r + a_1 T_r^{1.5} + a_2 T_r^{3}) \qquad (6)$$

was able to describe our data close to our estimated experimental uncertainty [dP = 0.021 and abs(dP) = 0.091], with the coefficients $a_0 = -7.8690$, $a_1 = 1.5448$, and $a_2 = -4.1836$. We found an error distribution close to the one presented in Figure 3.

Our experimental findings were also compared with values calculated using the MBWR EOS (McLinden et al., 1998); the results of the comparison are presented in Figure 4, showing good consistency down to 270 K.

Using the coefficients of the Antoine equation, eq 1, with the above-reported critical temperature and pressure values, we obtained the following value for the acentric factor, $\omega = 0.37758$.

***P*−*V*−*T*.** In Table 2, 42 experimental $P-V-T$ measurements in the superheated vapor region along seven isochores are presented. The measurements were taken in a density range from 0.17 to 0.39 mol dm^{-3} (26 to 59 kg m^{-3}) for temperatures from 314 K to 364 K and pressures from 406 kPa to 978 kPa.

Table 2. Experimental *P*−*V*−*T* Data for R-236fa

T_{90}/K	P/kPa	V/dm^3·mol^{-1}	T_{90}/K	P/kPa	V/dm^3 mol^{-1}
313.98	405.9	5.669	328.65	589.1	3.948
318.27	413.6	5.670	333.33	601.5	3.950
323.25	422.3	5.671	343.23	627.0	3.947
333.21	439.4	5.674	353.19	652.3	3.952
343.27	456.4	5.677			
353.17	472.9	5.680	331.78	688.9	3.305
362.15	487.7	5.682	338.77	712.4	3.306
			343.05	726.2	3.307
321.07	461.1	5.044	348.21	742.5	3.307
328.49	475.8	5.046	353.67	759.6	3.311
337.47	493.2	5.048			
346.20	509.8	5.050	338.64	765.4	2.991
353.47	523.5	5.052	344.07	785.0	2.992
358.37	532.6	5.053	348.07	799.2	2.993
363.98	543.1	5.054	354.08	820.2	2.993
			358.63	835.8	2.994
318.48	494.9	4.593	363.32	851.8	2.995
323.53	507.1	4.594			
328.18	517.5	4.595	343.45	890.8	2.560
333.20	528.5	4.596	348.33	911.8	2.560
338.19	539.3	4.597	353.49	933.6	2.561
343.18	550.1	4.598	358.64	955.3	2.562
348.53	561.6	4.599	363.97	977.7	2.562
353.62	572.3	4.601			

Second and Third Virial Coefficients. The experimental $P-V-T$ data were used to derive coefficients of the virial equation of state in the Leiden form, truncated after the third term,

$$P/\text{kPa} = \frac{RT/\text{K}}{V/\text{dm}^3\ \text{mol}^{-1}}\left(1 + \frac{B/\text{dm}^3\ \text{mol}^{-1}}{V/\text{dm}^3\ \text{mol}^{-1}} + \frac{C/\text{dm}^6\ \text{mol}^{-2}}{V^2/\text{dm}^3\ \text{mol}^{-1}}\right) \qquad (7)$$

where R = 8.31451 J mol^{-1} K^{-1} is the universal gas constant, V is the molar volume, B is the second virial coefficient, and C is the third virial coefficient. Considering that our $P-V-T$ data are isochoric but not isothermal, some empirical temperature relationship for $B(T)$ and $C(T)$ has to be assumed a priori. In addition, the temperature range of our $P-V-T$ data was not very wide, so we assumed some simple forms for the temperature dependence of B and C. In the outcome of regression using

$$Q = \sum_{i=1}^{n} (P_{\text{exp}} - P_{\text{calc}})^2/n \qquad (8)$$

as the objective function, we observed that the third virial coefficient values we found are heavily dependent on the algebraic form of the expressions used for the second virial coefficient, even if the objective function values found were very close. This is presumably due to fact that our experimental data cover a small pressure range and, in addition, a low reduced temperature range ($0.79 < T_r < 0.92$). As a result, we ultimately used the virial equation truncated after the second term along with the expression

$$B/\text{dm}^3\ \text{mol}^{-1} = B_0/\text{dm}^3\ \text{mol}^{-1} + \frac{B_1/\text{dm}^3\ \text{mol}^{-1}}{T/\text{K}} + (B_2/\text{dm}^3\ \text{mol}^{-1})\exp(1/T_r) \qquad (9)$$

where the coefficients B_i are $B_0 = 0.31004$, $B_1 = 880.577$,

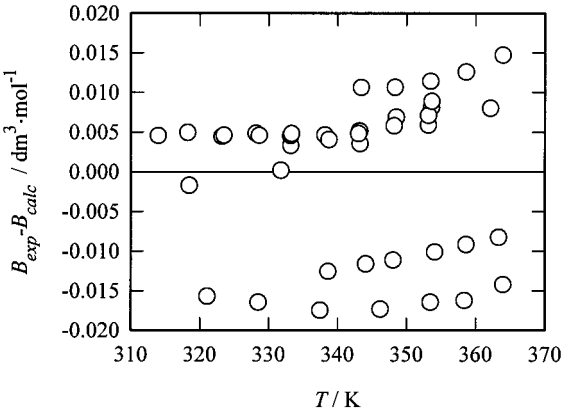

Figure 5. Scatter diagram of second virial coefficients from the fit with eq 9.

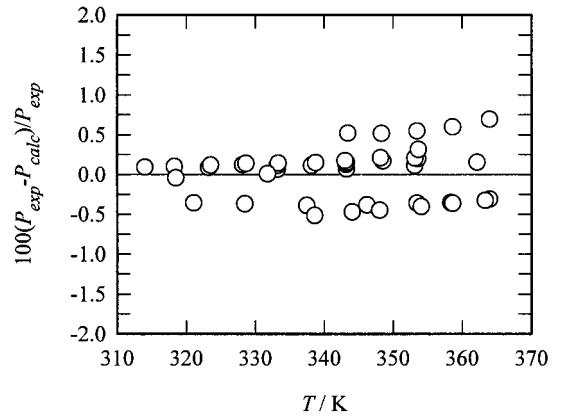

Figure 6. Scatter diagram of pressure deviations produced by the virial equation of state.

and $B_2 = -1.067$. The fit gives dP = 0.021 and abs(dP) = 0.264, both as percentages. The deviations between the second virial coefficients by eq 9 and those derived from experimental data are shown in Figure 5. Using eq 7 with the experimental temperature and volume data, and with the coefficients specified above for B, the deviations from the experimental pressure defined as

$$dP_i = (P_{i,\mathrm{exp}} - P_{i,\mathrm{calc}})/P_{i,\mathrm{exp}} \times 100 \qquad (10)$$

were calculated for each data point and are presented in Figure 6. The deviations absorb both the experimental uncertainties in the measured quantities and those coming from the assumed empirical relation of eq 9.

To our knowledge, the second virial coefficients of highly fluorinated propane derivatives have not been compared with the correlating equations, so we compared them, choosing the Tsonopoulos method (Tsonopoulos, 1974), the O'Connell and Prausnitz method (O'Connell and Prausnitz, 1967), and the method recently proposed by Weber for small, polar molecules (Weber, 1994). It should be pointed out that this last method was validated for the methane and ethane halo (F and Cl) derivatives. All methods are basically derived from the Pitzer and Curl (1957) idea, and the Weber method is a modification of the Tsonopoulos method. The additional quantities that were needed for all methods were the dipole moment, μ = 1.982 D (Goodwin and Mehl, 1997), and the reduced dipole moment μ_R,

$$\mu_R = (1 \times 10^5)(\mu^2/\mathrm{D})(P_c/\mathrm{atm})/(T_c^2/\mathrm{K}) = 78.2 \qquad (11)$$

In addition, for the O'Connell and Prausnitz method, we

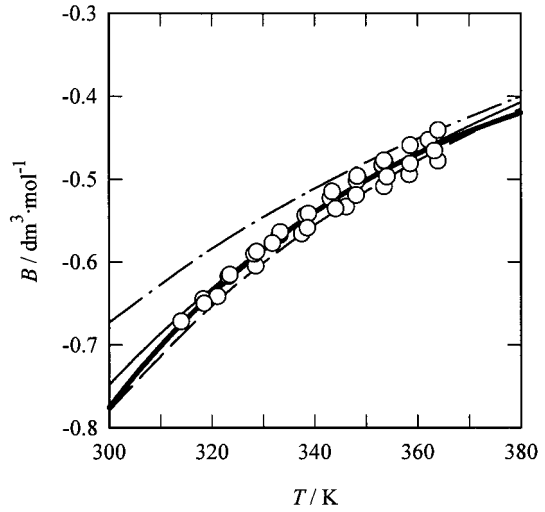

Figure 7. Second virial coefficients derived from the $P-V-T$ data (○), their representation with the coefficients of eq 5 (thick line), and predicted by the O'Connell and Prausnitz (dash and dot line), the Tsonopoulos (thin line), and the Weber (dashed line) correlating methods.

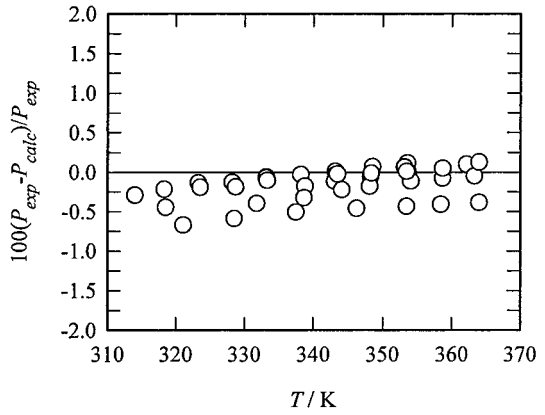

Figure 8. Scatter diagram of deviations between experimental $P-V-T$ data and values calculated with the MBWR EOS (McLinden et al., 1998).

considered propane with its acentric value ω = 0.153 (Reid et al., 1987) as a homomorph of R236fa, although, having the same number of segments, they are naturally different in size. The results are shown in Figure 7, which demonstrates good consistency of the derived second virial coefficients from the $P-V-T$ measurements with the Tsonopoulos (1974) and the Weber (1994) correlating methods. Our results for $P-V-T$ were also compared with density values calculated using the MBWR EOS (McLinden et al., 1998); the resulting deviations are presented in Figure 8, again showing good consistency.

Conclusions

The present work presents 113 experimental data points for saturated pressure and the superheated region of R-236fa, obtained using the constant volume apparatus. The refrigerant's behavior along the saturation line is described by 71 experimental points, and 42 experimental points describe its $P-V-T$ behavior along seven isochores in the superheated vapor region. Data collected for the saturated pressure were correlated with a few empirical equations with three or four adjustable parameters. The best representation of the experimental results was found with the four-parameter equation of the Antoine type. The $P-V-T$ data in the superheated region were fitted to the

virial equation of state. We were unable to derive the third virial coefficients successfully (presumably due to the small pressure range and small reduced temperatures of our data), but the $P-V-T$ data are well represented by the virial equation of state truncated after the second term. The consistency of the derived second virial coefficients with the Tsonopoulos and the Weber correlating methods is very good. The consistency of both experimental saturated pressure and $P-V-T$ data and those calculated using the MBWR EOS is also good.

Literature Cited

Basile, G. Ausimont spa, private communication, 1998.

Beyerlein, A. L.; DesMarteau, D. D.; Hwang, S. H.; Smith, N. D.; Joyner, P. Physical properties of fluorinated propane and butane derivatives as alternative refrigerants. *ASHRAE Trans.*; 1993; part 1, pp 368−379.

Bobbo, S.; Stryjek, R.; Elvassore, N.; Bertucco, A. A recirculation apparatus for vapor-liquid equilibrium measurements of refrigerants. Binary mixtures of R600a, R134a and R236fa. *Fluid Phase Equilib.* **1998**, *150*, 343−352.

Gillis, K. A. Thermodynamic properties of seven gaseous halogenated hydrocarbons from acoustic measurements: $CHClFCF_3$, CHF_2CF_3, CF_3CH_3, CH_2CH_3, $CF_3CHFCHF_2$, $CF_3CH_2CF_3$, and $CHF_2CF_2CH_2F$. *Int. J. Thermophys.* **1997**, *18*, 73−135.

Giuliani, G.; Kumar, S.; Zazzini, P.; Polonara, F. Vapor pressure and gas-phase PVT data and correlation for 1,1,1-trifluoroethane (R143a). *J. Chem. Eng. Data* **1995**, *40a*, 903−908.

Giuliani, G.; Kumar, S.; Polonara, F. A constant volume apparatus for vapour pressure and gas-phase P−v-T measurements: validation with data for R22 and R134a. *Fluid Phase Equilib.* **1995**, *109b*, 265−279.

Goodwin, A. R. H.; Mehl, J. B. Measurements of dipole moments of seven partially fluorinated hydrocarbons with a radio frequency reentrant cavity resonator. *Int. J. Thermophys.* **1997**, *18*, 795−806.

Hwang, S. H.; DesMarteau, D. D.; Beyerlein, A. L.; Smith, N. D.; Joyner, P. The heat capacity of fluorinated propane and butane derivatives by differential scanning calorimetry. *J. Therm. Anal.* **1992**, *38*, 2515−2528.

Laesecke, A.; Defibaugh, D. R. Viscosity of 1,1,1,2,3,3-hexafluoropropane and 1,1,1,3,3,3-hexafluoropropane at saturated-liquid conditions from 262 K to 353 K. *J. Chem. Eng. Data* **1996**, *41*, 59−62.

McLinden, M. O.; Klein, S. A.; Lemmon, E. W.; Peskin, A. P. *NIST thermodynamic and transport properties of refrigerants and refrigerant mixture (REFPROP)*, version 6.0; Natl. Inst. of Standards and Technology, Physical and Chemical Properties Division: Boulder, CO, 1998.

O'Connell, J. P.; Prausnitz, J. M. Empirical correlation of second virial coefficients for vapor-liquid equilibrium calculations. *Ind. Eng. Chem., Process Des. Dev.* **1967**, *6*, 245−250.

Outcalt, S. L.; McLinden, M. O. An equation of state for the thermodynamic properties of R236fa; NIST report, 1995, N61533-94-F-0152.

Reid, R. C.; Prausnitz, J. M.; Poling, B. E. *The properties of gases & liquids*, 4th ed.; McGraw-Hill: New York, 1987.

Schmidt, J. W.; Carrillo-Nava, E.; Moldover, M. R. Partially halogenated hydrocarbons $CHFCl-CF_3$, CF_3-CH_3, $CF_3-CHF-CHF_2$, $CF_3-CH_2-CF_3$, $CHF_2-CF_2-CH_2F$, $CF_3-CH_2-CHF_2$, $CF_3-O-CHF_2$: critical temperature, refractive indices, surface tension and estimates of liquid, vapor and critical densities. *Fluid Phase Equilib.* **1996**, *122*, 187−206.

Setzmann, U.; Wagner, W. A new equation of state and tables of thermodynamic properties for methane covering the range from the melting line to 625 K at pressures up to 1000 MPa. *J. Phys. Chem. Ref. Data* **1991**, *20*, 1061−1155.

Tsonopoulos, C. An empirical correlation of second virial coefficients, *AICHE J.* **1974**, *20*, 263−272.

Weber, L. A. Estimating the virial coefficients of small polar molecules. *Int. J. Thermophys.* **1994**, *15*, 461−482.

Received for review November 24, 1998. Accepted March 17, 1999. This work was supported by the European Union as part of the Joule Project within the IV Framework for RTD, and by the Italian Ministero dell'Università e della Ricerca Scientifica e Tecnologica.

JE980281E